LETTER

Disease associations between honeybees and bumblebees as a threat to wild pollinators

M. A. Fürst[1,2], D. P. McMahon[3], J. L. Osborne[4,5], R. J. Paxton[3,6,7] & M. J. F. Brown[1]

Emerging infectious diseases (EIDs) pose a risk to human welfare, both directly[1] and indirectly, by affecting managed livestock and wildlife that provide valuable resources and ecosystem services, such as the pollination of crops[2]. Honeybees (*Apis mellifera*), the prevailing managed insect crop pollinator, suffer from a range of emerging and exotic high-impact pathogens[3,4], and population maintenance requires active management by beekeepers to control them. Wild pollinators such as bumblebees (*Bombus* spp.) are in global decline[5,6], one cause of which may be pathogen spillover from managed pollinators like honeybees[7,8] or commercial colonies of bumblebees[9]. Here we use a combination of infection experiments and landscape-scale field data to show that honeybee EIDs are indeed widespread infectious agents within the pollinator assemblage. The prevalence of deformed wing virus (DWV) and the exotic parasite *Nosema ceranae* in honeybees and bumblebees is linked; as honeybees have higher DWV prevalence, and sympatric bumblebees and honeybees are infected by the same DWV strains, *Apis* is the likely source of at least one major EID in wild pollinators. Lessons learned from vertebrates[10,11] highlight the need for increased pathogen control in managed bee species to maintain wild pollinators, as declines in native pollinators may be caused by interspecies pathogen transmission originating from managed pollinators.

Trading practices in domesticated animals enable infectious diseases to spread rapidly and to encounter novel hosts in newly sympatric wildlife[12]. This 'spillover' of infectious disease from domesticated livestock to wildlife populations is one of the main sources of emerging infectious disease (EID)[13]. Small or declining populations are particularly challenged, as the source host may act as a disease reservoir[14], giving rise to repeated spillover events and frequent disease outbreaks that, in the worst case, might drive already vulnerable or unmanaged populations to extinction[14]. Such severe impacts have been well documented over the past decades in vertebrates[10], but have largely been overlooked in invertebrates[15]. Recent years have seen elevated losses in multiple populations of one of the major crop-pollinating insects, the honeybee (*Apis mellifera*)[16]. EIDs have been suggested as key drivers of decline, and deformed wing virus (DWV) (particularly in combination with the exotic *Varroa* mite (*Varroa destructor*)) and *Nosema ceranae* are two likely causes for losses of honeybees[17]. As generalist pollinators, honeybees are traded and now distributed almost worldwide for crop pollination and hive products. They share their diverse foraging sites with wild pollinators and thus facilitate interspecific transmission of pathogens, as has been suggested for intraspecific disease transmission from commercial to wild bumblebee populations[18]. Our focus is on interspecific transmission, as EIDs in managed honeybees are a potential threat to a range of wild pollinators worldwide. Although evidence from small-scale studies suggests that wild pollinators like *Bombus* spp. may already harbour some honeybee pathogens[7,8,19,20], the true infectivity and landscape-scale distribution of these highly virulent EIDs in wild pollinator populations remains unknown.

To examine the potential for *Apis* pathogens to cross host–genus boundaries, we tested the infectivity of the DWV complex (which includes the very closely related, co-occurring and recombinant *Varroa destructor* virus (VDV)[21,22]; we will refer to the DWV complex as 'DWV' throughout the text) and *N. ceranae*, in controlled inoculation experiments, to one of the most common *Bombus* species in the United Kingdom (*B. terrestris*). DWV is infective for *B. terrestris*; we found significantly more DWV infections 21 days after inoculating *B. terrestris* workers versus controls (likelihood ratio test comparing the full model to one with only the intercept: $X^2 = 5.73$, d.f. $= 1$, $P < 0.017$; Fig. 1) and mean survival was reduced by 6 days. As for *Apis,* DWV causes deformed wings in *Bombus* when overtly infected[8], resulting in non-viable offspring and reduced longevity (Fig. 1). *N. ceranae* is also infective for *B. terrestris*; infections increased in *Bombus* versus control ($X^2 = 17.76$, d.f. $= 1$, $P < 0.001$; Fig. 1), although overt symptoms were not seen (mean survival increased by 4 days).

After we established that both DWV and *N. ceranae* are infective for *B. terrestris*, we conducted a structured survey across 26 sites in Great Britain and the Isle of Man (see Extended Data Fig. 1). We collected 10 *Apis* samples and 20 *Bombus* samples per site to assess EID prevalence (for details on the species identity across sites, see Extended Data Fig. 1). We analysed a total of 745 bees from 26 sites for DWV presence, DWV infection (replicating DWV) and *N. ceranae* presence. DWV was present in 20% (95% confidence interval (CI), 17–23%) of all samples; 36% (95% CI, 30–43%) of *Apis* and 11% (95% CI, 9–15%) of *Bombus*. Of the *Apis* harbouring DWV, 88% (95% CI, 70–98%) of the samples tested had actively replicating virus, whereas 38% (95% CI, 25–53%) of *Bombus* harbouring DWV had replicating virus (see Extended Data Fig. 2 and Extended Data Table 1). *N. ceranae* was less frequent, being detected in 7% (95% CI, 6–10%) of all samples; 9% (95% CI, 6–13%) of *Apis* samples and 7% (95% CI, 5–9%) of *Bombus* samples.
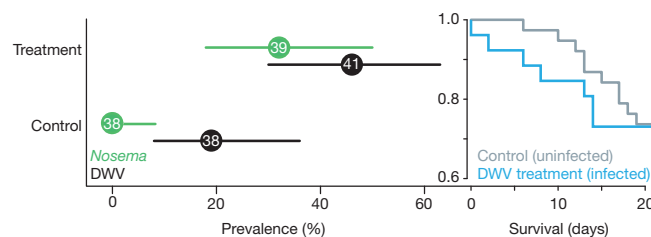

Figure 1 | DWV and *N. ceranae* infectivity in bumblebees. Prevalence of infections in treated *Bombus terrestris* workers 21 days after inoculation. Bars indicate 95% confidence intervals. Green, *Nosema*-treated samples; black, DWV-treated samples. Sample sizes are given inside the mean data point. The survival graph over the 21-day test period shows uninfected control treatments in grey compared to infected DWV treatments in blue (Cox mixed-effects model fitted with penalized partial likelihood: $X^2 = 11.93$, d.f. $= 4.17$; $P < 0.021$, see Methods) (*y* axis shows survival probability).

[1]Royal Holloway University of London, School of Biological Sciences, Bourne Building, Egham TW20 0EX, UK. [2]IST Austria (Institute of Science and Technology Austria), 3400 Klosterneuburg, Austria. [3]Queen's University Belfast, School of Biological Sciences, 97 Lisburn Road, Belfast BT9 7BL, UK. [4]Rothamsted Research, Department of Agro-Ecology, Harpenden AL5 2JQ, UK. [5]University of Exeter, Environment & Sustainability Institute, Penryn TR10 9EZ, UK. [6]Martin-Luther-Universität Halle-Wittenberg, Institute for Biology/General Zoology, Hoher Weg 8, 06120 Halle (Saale), Germany. [7]German Centre for Integrative Biodiversity Research (iDiv), Halle-Jena-Leipzig, Deutscher Platz 5e, 04103 Leipzig, Germany.

DWV-present *Apis* DWV-present *Bombus* DWV-replicating *Bombus* *Nosema ceranae* in *Apis* *Nosema ceranae* in *Bombus*
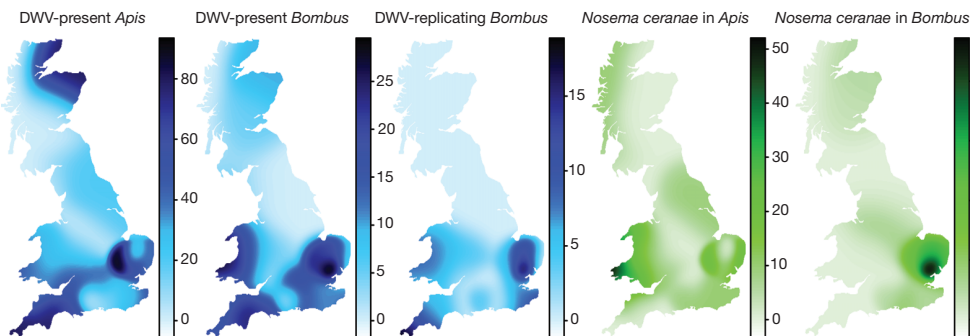
Figure 2 │ Geographical distribution of DWV and *N. ceranae* across their pollinator hosts. Estimated pathogen prevalence in *Apis* and *Bombus* across Great Britain. Colour gradient (based on Gaussian kernel estimators with an adaptive bandwidth of equal number of observations over 26 sites, see Methods) corresponds to per cent prevalence (note different scales). DWV prevalence is displayed in blue and *Nosema* prevalence in green.

We estimated the Great-Britain-wide prevalence of the two pathogens in *Apis* and *Bombus* spp. based on our field survey data (Fig. 2). We found no evidence for spatial clustering of DWV presence in *Bombus* (Moran's $I = 0.023$, $P > 0.211$) or either of the pathogens in *Apis* (DWV presence: Moran's $I = 0.03$, $P > 0.186$; *Nosema* presence: Moran's $I = -0.061$, $P > 0.649$). However, there was weak clustering of DWV infection in *Bombus* (Moran's $I = 0.061$, $P < 0.044$) and very strong clustering of *N. ceranae* in *Bombus* (Moran's $I = 0.25$, $P < 0.001$), indicating disease hotspots for DWV in *Bombus* in the south west and east of Great Britain and for *N. ceranae* in *Bombus* in the south east of Great Britain (Fig. 2). As prevalence was lower in *Bombus* than *Apis*, we modelled pathogen prevalence in *Bombus* as dependent on pathogen prevalence in *Apis*, *Apis*:*Bombus* (ratio of host densities) and *Apis* abundance, including biologically relevant interactions while controlling for latitude, longitude and sunlight hours, and adding collection site and species identity as random factors. Our full model for DWV presence fitted the data significantly better than the null model without any of the test predictors and their interactions included (likelihood ratio test: $X^2 = 19.03$, d.f. = 5, $P < 0.002$). After removal of the non-significant interactions (general linear mixed model (GLMM): *Bombus*:*Apis* × DWV presence in *Apis*, estimate ± s.e. of the estimate of the fixed effect parameter in the model = -0.105 ± 1.376, $P = 0.939$; *Apis* abundance × DWV presence in *Apis*, 0.425 ± 1.309, $P = 0.745$), it is clear that prevalence of DWV in *Apis* has a strong positive effect on DWV prevalence in *Bombus* (GLMM: 2.718 ± 0.921, $z = 2.951$, $P < 0.004$) (Fig. 2, and Extended Data Fig. 3), whereas none of the other predictors had a role (GLMM: *Bombus*:*Apis*, 0.315 ± 0.387, $z = 0.814$, $P < 0.416$; *Apis* abundance, -0.085 ± 0.364, $z = -0.232$, $P < 0.816$). In the case of *N. ceranae*, our full model fitted the data significantly better than the null model ($X^2 = 15.8$, d.f. = 5, $P < 0.008$). Specifically, there was an effect of *Nosema* prevalence in *Apis* on *Nosema* prevalence in *Bombus* and this varied with *Apis* abundance (interaction between *Nosema* prevalence in *Apis* and *Apis* abundance, $X^2 = 7.835$, d.f. = 2, $P < 0.02$), whereas *Bombus*:*Apis* did not explain *Nosema* prevalence in *Bombus* (GLMM: 8.386 ± 6.793, $z = 1.235$, $P = 0.217$) (Fig. 2 and Extended Data Fig. 3).

The prevalence data implied local transmission of DWV between *Apis* and *Bombus*. To test this, we sequenced up to five isolates per DWV infected *Bombus* sample from five sites matched by up to five isolates of sympatric DWV infected *Apis* samples. If a pathogen is transmitted between these two hosts, we would expect *Apis* and *Bombus* to share the same DWV strain variants within a site. Marginal log likelihoods estimated by stepping stone sampling[23] decisively supported clades constrained by site as opposed to host, indicating pathogen transmission within site (Fig. 3 and Extended Data Table 2).

Our results provide evidence for an emerging pathogen problem in wild pollinators that may be driven by *Apis*. Our data cannot demonstrate directionality in the interspecific transmission of DWV. However, the high prevalence of DWV in honeybees, which is a consequence of the exotic vector *Varroa destructor*[24], is consistent with the hypothesis

that they are the major source of infection for the pollinator community. Similar results have been found for intraspecific transmission of *Bombus*-specific pathogens from high prevalence commercial *Bombus* colonies to low prevalence wild *Bombus* populations[18]. Our field estimates
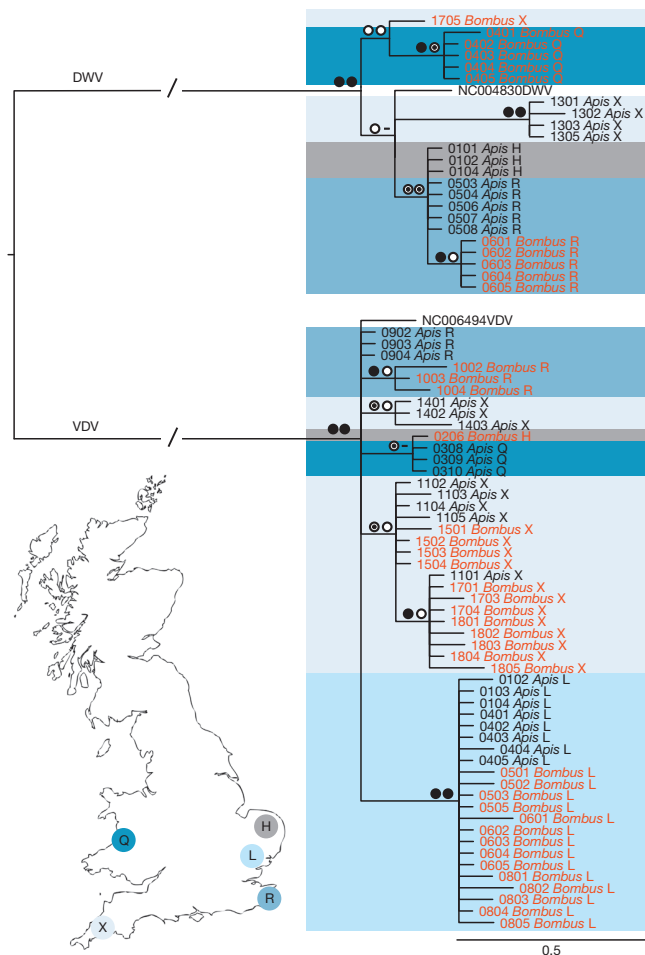

Figure 3 │ Sympatric *Apis* and *Bombus* share viral strains. RNA-dependent RNA polymerase partial gene phylogeny of pollinator viruses (see main text). Gene trees were estimated using PhyML v.3.0 maximum-likelihood (ML) bootstrapping (500 replicates) and MrBayes v3.2.1 (see Methods). Coloured boxes correspond to sites H, L, Q, R and X (as shown on the map) and text colours correspond to host (red, *Bombus*; black, *Apis*). Symbols represent node support values: posterior probability (left), bootstrap support (right). Filled circle, >90%; target symbol, >70%; empty circle, >50%; hyphen, <50%. Branches (/), one-third of true length. Numbers are IDs; first two numbers represent the individual, second two numbers represent the clone.

of prevalence are conservative for DWV, as highly infected individuals have deformed wings, are incapable of flight, and thus would not be captured by our sampling protocol. Consequently, DWV prevalence and, as a result, impact are likely to be higher in managed and wild populations than our data suggest. Interestingly, *N. ceranae* prevalence in *Bombus* depends positively on *Apis* abundance, but only when *N. ceranae* prevalence in *Apis* is low, suggesting a possible environmental saturation effect of *N. ceranae* spores. In contrast to the low impact of *N. ceranae* on the survival of *B. terrestris* in our study, very high virulence was found by another study[25]. This might be explained by our use of young bees compared to the non-age-controlled design used in the other paper[25], indicating age-dependent differential susceptibility in *B. terrestris,* as has been suggested to be the case in honeybees[26].

Ongoing spillover of EIDs could represent a major cause of mortality of wild pollinators wherever managed bees are maintained. Although our data are only drawn from Great Britain, the prerequisites for honeybees to be a source or reservoir for these EIDs—high colony densities and high parasite loads—are present at a global scale. In addition, global trade in both honeybees and commercial *Bombus* may exacerbate this impact[6,27]. Reducing the pathogen burden in managed honeybees so as to reduce the risk of transmission to wild pollinators is not straightforward. Tighter control of importation and hygiene levels of transported colonies could be imposed with regulation, but policies developed in this direction must learn from the past; such regulation is difficult to implement and hard to evaluate[9,28]. Clearly, it is essential to ensure that those managing bees (including commercial producers, growers and beekeepers) have access to the methods and skills to monitor, manage and control EIDs for the benefit of their managed colonies, and the wider pollinator community. A consensus on the threat of EIDs for wild pollinators can only be reached with greater knowledge of their epidemiology, global extent and impact, and it will be crucial to involve key stakeholders (for example, the beekeeping community, *Bombus* exporters) in any decision process, as any progress made will largely be driven by their actions.

METHODS SUMMARY

Bombus inoculation experiment. Two-day-old workers of *Bombus terrestris audax* colonies (Biobest) were individually inoculated with either 10^5 spores per bee purified *N. ceranae* or 10^9 genome equivalents per bee purified DWV in 10 μl sucrose solution. Bees surviving for 21 days were freeze-killed and tested for pathogen presence using molecular techniques.

Sampling scheme. Sampling took place at 24 mainland sites and 2 islands, Colonsay and the Isle of Man, which are currently free of *Varroa destructor* (the main vector for DWV in *Apis mellifera*) (see Extended Data Fig. 1 for site distribution). Cryptic *Bombus* species were identified by PCR–RFLP (restriction fragment length polymorphism) analysis. *Apis* and *Bombus* densities were estimated for each site by timing the collection effort for 20 samples from each genus simultaneously. Samples collected were freeze-killed at $-20\,^\circ$C and transferred to $-80\,^\circ$C as soon as possible thereafter. RNA and DNA preparation and virus strand specific PCR with reverse transcription (RT–PCR) followed standard protocols.

Statistics. True prevalences with 95% confidence intervals were computed with the function epi.prev in the R library epiR, version 0.9-45.

Overall prevalence for each of our parasites was calculated using Gaussian kernel estimators with an adaptive bandwidth of equal number of observations (set to 3× the maximum observations per site) (R library prevR, version 2.1, function kde).

Moran's *I* was calculated as implemented in the R library package ape (version 3.0-7, function Moran.I).

We ran GLMMs to investigate both effects on disease status of individuals 21 days after pathogen challenge and also pathogen prevalence in *Bombus* using the function lmer of the R package lme4. All analyses were run in R.

Online Content Any additional Methods, Extended Data display items and Source Data are available in the online version of the paper; references unique to these sections appear only in the online paper.

Received 21 October; accepted 30 December 2013.

1. Binder, S., Levitt, A. M., Sacks, J. J. & Hughes, J. M. Emerging infectious diseases: public health issues for the 21st century. *Science* **284**, 1311–1313 (1999).
2. Oldroyd, B. P. Coevolution while you wait: *Varroa jacobsoni*, a new parasite of western honeybees. *Trends Ecol. Evol.* **14**, 312–315 (1999).
3. Ratnieks, F. L. W. & Carreck, N. L. Clarity on honey bee collapse? *Science* **327**, 152–153 (2010).
4. Vanbergen, A. J. & The Insect Pollinator Initiative. Threats to an ecosystem service: pressures on pollinators. *Front. Ecol. Environ* **11**, 251–259 (2013).
5. Williams, P. H. & Osborne, J. L. Bumblebee vulnerability and conservation world-wide. *Apidologie* **40**, 367–387 (2009).
6. Cameron, S. A. *et al.* Patterns of widespread decline in North American bumble bees. *Proc. Natl Acad. Sci. USA* **108**, 662–667 (2011).
7. Evison, S. E. F. *et al.* Pervasiveness of parasites in pollinators. *PLoS ONE* **7**, e30641 (2012).
8. Genersch, E., Yue, C., Fries, I. & de Miranda, J. R. Detection of deformed wing virus, a honey bee viral pathogen, in bumble bees (*Bombus terrestris* and *Bombus pascuorum*) with wing deformities. *J. Invertebr. Pathol.* **91**, 61–63 (2006).
9. Meeus, I., Brown, M. J. F., De Graaf, D. C. & Smagghe, G. Effects of invasive parasites on bumble bee declines. *Conserv. Biol.* **25**, 662–671 (2011).
10. Fisher, M. C. *et al.* Emerging fungal threats to animal, plant and ecosystem health. *Nature* **484**, 186–194 (2012).
11. Krebs, J. *et al.* Bovine Tuberculosis in Cattle and Badgers (MAFF Publications, 1997).
12. Vitousek, P. M., Dantonio, C. M., Loope, L. L. & Westbrooks, R. Biological invasions as global environmental change. *Am. Sci.* **84**, 468–478 (1996).
13. Daszak, P. Emerging infectious diseases of wildlife — threats to biodiversity and human health. *Science* **287**, 443–449 (2000).
14. Dobson, A. Population dynamics of pathogens with multiple host species. *Am. Nat.* **164**, S64–S78 (2004).
15. Alderman, D. J. Geographical spread of bacterial and fungal diseases of crustaceans. *Rev. Sci. Tech.* **15**, 603–632 (1996).
16. Neumann, P. & Carreck, N. L. Honey bee colony losses. *J. Apic. Res.* **49**, 1–6 (2010).
17. Paxton, R. J. Does infection by *Nosema ceranae* cause ''Colony Collapse Disorder'' in honey bees (*Apis mellifera*)? *J. Apic. Res.* **49**, 80–84 (2010).
18. Murray, T. E., Coffey, M. F., Kehoe, E. & Horgan, F. G. Pathogen prevalence in commercially reared bumble bees and evidence of spillover in conspecific populations. *Biol. Conserv.* **159**, 269–276 (2013).
19. Singh, R. *et al.* RNA viruses in Hymenopteran pollinators: evidence of inter-taxa virus tansmission via pollen and potential impact on non-*Apis* Hymenopteran species. *PLoS ONE* **5**, e14357 (2010).
20. Graystock, P. *et al.* The Trojan hives: pollinator pathogens, imported and distributed in bumblebee colonies. *J. Appl. Ecol.* **50**, 1207–1215 (2013).
21. Ongus, J. R. *et al.* Complete sequence of a picorna-like virus of the genus Iflavirus replicating in the mite *Varroa destructor*. *J. Gen. Virol.* **85**, 3747–3755 (2004).
22. Moore, J. *et al.* Recombinants between deformed wing virus and *Varroa destructor* virus-1 may prevail in *Varroa destructor*-infested honeybee colonies. *J. Gen. Virol.* **92**, 156–161 (2011).
23. Xie, W., Lewis, P. O., Fan, Y., Kuo, L. & Chen, M.-H. Improving marginal likelihood estimation for Bayesian phylogenetic model selection. *Syst. Biol.* **60**, 150–160 (2011).
24. Martin, S. J. *et al.* Global honey bee viral landscape altered by a parasitic mite. *Science* **336**, 1304–1306 (2012).
25. Graystock, P., Yates, K., Darvill, B., Goulson, D. & Hughes, W. O. H. Emerging dangers: deadly effects of an emergent parasite in a new pollinator host. *J. Invertebr. Pathol.* **114**, 114–119 (2013).
26. Smart, M. D. & Sheppard, W. S. *Nosema ceranae* in age cohorts of the western honey bee (*Apis mellifera*). *J. Invertebr. Pathol.* **109**, 148–151 (2012).
27. Otterstatter, M. C. & Thomson, J. D. Does pathogen spillover from commercially reared bumble bees threaten wild pollinators? *PLoS ONE* **3**, (2008).
28. Donnelly, C. A. & Woodroffe, R. Reduce uncertainty in UK badger culling. *Nature* **485**, 582 (2012).

Author Contributions The study was jointly conceived by R.J.P., J.L.O. and M.J.F.B. Experiments were designed by M.A.F. and M.J.F.B.; M.A.F prepared the manuscript; M.J.F.B., D.P.M., R.J.P. and J.L.O. edited the manuscript. M.A.F. carried out the experimental, molecular work and analyses, and D.P.M. undertook the phylogenetic analyses.

METHODS

***Bombus* inoculation experiment.** Each of the seven experimental *Bombus terrestris* colonies (Biobest) was tested for the presence of the two treatment pathogens DWV and *N. ceranae*. Daily, callows (newly emerged workers) were removed from the colony, assigned sequentially to random treatment blocks and housed individually in small Perspex boxes on an *ad libitum* diet of 50% sucrose solution and artificial pollen (Nektapoll), as natural pollen has been shown to contain viable *N. ceranae* spores and DWV virions[19,29]. Two-day-old bumblebee workers were individually inoculated with a treatment-dependent inoculum in 10 µl sucrose. Crude hindgut extracts of five *Apis* workers propagating *N. ceranae* were purified by the triangulation method[30] with slight adaptations.

We used small cages with 30 *N. ceranae* infected honeybees to propagate *N. ceranae* spores for the inoculum. Every second day we collected five honeybees from these cages, and removed and ground the hindguts. The resulting extract was filtered through cotton and washed with 0.9% insect ringer (Sigma Aldrich). We triangulated extracts using Eppendorf tubes and spin speeds of 0.5 RCF (relative centrifugal force) for 3 min, purifying *N. ceranae* spores across a series of seven tubes. Spore numbers were quantified in a Neubauer counting chamber. In parallel, we extracted and purified *N. ceranae* free bees to use for control inoculations.

DWV virus inoculum was prepared according to a previous paper[31] but with modifications. Honeybees with DWV symptoms (crippled wings and body deformities) were crushed in 0.5 M potassium phosphate buffer, pH 8.0, filtered and clarified by slow-speed centrifugation (8,000*g* for 10 min) before being diluted and injected (1 µl) into white-eyed pupae for bulk propagation of virus. After 5 days, up to 100 pupae were harvested, and after a screen by quantitative RT–PCR (qRT–PCR), virus was purified. Virus extraction buffer consisted of 0.5 M potassium phosphate pH 8.0, 0.2% DEICA, 10% diethyl ether. Purification consisted of two slow-speed clarifications (8,000*g* for 10 min), one high-speed clarification (75,000*g* for 3 h) followed by re-suspension in 0.5 M potassium phosphate buffer (pH 8.0) and a final slow speed clarification. Virus preparations were aliquoted and stored at −80 °C until use in inoculation experiments.

Quantitative RT-PCR was used to check the purified virus for presence of DWV and absence of other common honeybee RNA viruses: ABPV (acute bee paralysis virus), BQCV (black queen cell virus), CBPV (chronic bee paralysis virus), IAPV (Israeli acute paralysis virus), SBV (sacbrood virus) and SBPV (slow bee paralysis virus).

A duplicate dilution series of external DNA standards covering 10^2 to 10^8 molecules (reaction efficiencies: 90–110%, r^2: 0.95–0.99) were included in qRT–PCR runs to quantify DWV genome equivalents present in the inoculum. For absolute quantification of virus dose, an external DNA standard was generated by amplifying a genomic fragment of 241 bp using the primers F8668*std* (5′-GATGGG TTTGATTCGATATCTTGG-3′) and B8757*std* (5′-GGCAAACAAGTATCTTT CAAACAATC-3′) via RT–PCR that contained the 136-bp fragment amplified by the DWV-specific qRT–PCR primers F8668 and B8757 (ref. 32).

Shortly before administration, inocula were prepared to a total concentration of 10^5 spores per bee in 10 µl (10^4 spores per µl sucrose solution). Inocula were administered individually in a small Petri dish after 30–60 min starvation. Only workers ingesting the full 10 µl within 1 h were used in the experiment.

Sampling scheme. The mainland sampling sites were chosen across Great Britain along a north–south transect (12 sampling points with fixed latitude, but free in longitude) and across two east–west transects (12 sampling points with fixed longitude, but free within a narrow latitudinal corridor). Each of the mainland sites were at least 30 km apart (mean ± s.d. of nearest neighbour = 69.21 ± 26.39). The island sites were chosen deliberately to gain background data for both *Apis* and *Bombus* disease prevalence in the absence of *Varroa*, the main transmission route for DWV in *Apis*. At each sampling site we collected approximately 30 workers for each of the following species: *Apis mellifera*, *Bombus terrestris* (verified by RFLP analysis[33]), and the next most common bumblebee on site. We collected free-flying bees from flowers rather than bees from colonies as this is the most likely point of contact in the field. By collecting from flowers we lowered the likelihood of collecting bumblebees from different colonies. Although we ran the risk of collecting multiple honeybees from the same hive, this nevertheless represents the potential force of infection for both genera in the field.

Each collection took place along a continuous transect, where maximally 10 bees per 10-m stretch were collected before moving on to the next ten metre stretch. At each site, the collection area covered at least 1000 m² (for example, 1000 m, 20 × 50 m). Each sampling point was within one of the following landcover types: urban areas (gardens and parks), farmland (hedgerows, border strips, crops and wildflower meadows), coastal cliffs, sand dunes and heather moorland.

If possible, we collected all bees within a single day. In the case of adverse weather, we returned as soon as possible to finish the collection at the exact same site. To estimate *Apis* and *Bombus* densities at each site we timed the collection effort simultaneously. Time taken to collect 20 *Bombus* workers (of any *Bombus* species)

and 20 *Apis* workers was recorded, respectively. Timed collecting efforts took place on a single day only.

Samples collected were put in sampling tubes, transferred straight onto ice, then freeze-killed at −20°C and transferred to −80°C as soon as possible thereafter to ensure optimal RNA (DWV) preservation.

RNA work. RNA extraction followed the standard RNeasy plant mini kit (Qiagen) protocol with the final elutate (in RNase free ddH2O) of 30 µl being run over the column twice (for optimal RNA concentration). For reverse transcription of RNA to complementary DNA we followed the standard protocol of the Nanoscript Kit (Primerdesign). Our priming was target specific in separate reactions for *N. ceranae* (primer pair *N. ceranae*[34]), DWV (primer pair F15–B23 (ref. 35)) and a house-keeping gene (primer pair ACTB[36]) as a positive control for RNA extraction efficiency. Bees were transferred to liquid N_2 before dissection. Each bee's abdomen was cut with a sterile scalpel dorsoventrally along the sagittal plane. One half was submerged in RLT buffer (Qiagen) for RNA extraction, and the second half was archived at −80 °C. Tissue disruption and homogenization of individual half-abdomens was performed on a tissue lyser II (Qiagen) at 30 Hz for 2 min followed by 20 Hz for 2 min. RNA quality and quantity were checked on a Spectrometer (Nanodrop, Thermo Scientific). cDNA preparation was conducted at 65 °C for 5 min for the initial priming immediately before the addition of the reverse transcriptase. For the extension, samples were incubated at 25 °C for 5 min followed by 55 °C for 20 min and then heat inactivated for 15 min at 75 °C. cDNA was used as template in a standard PCR with 57 °C, 54 °C and 57 °C annealing temperatures, respectively. Results were visualized on a 2% agarose gel with ethidium bromide under ultraviolet light. Agarose gels were scored without knowledge of sample ID. To verify the specificity of the amplicon, one purified PCR product taken from *Apis* and one taken from *B. lapidarius* were sequenced (Macrogen).

Detection of negative-strand DWV. Detection of pathogens in pollinators in the field does not provide proof of infection, as pathogens are likely to be ingested on shared, contaminated food resources and therefore are inevitably present in the gut lumen as passive contaminants without necessarily infecting the host. To minimize these cases, we tested all of our DWV positive *Bombus* samples and a subset of DWV positive *Apis* samples for virus replication, a strong indicator for infection[37]. DWV is a positive strand virus whose negative strand is only present in a host once the virus is actively replicating[31]. Reverse transcription was conducted using a tagged primer tagB23 (ref. 38) for the initial priming to target exclusively the negative strand. The resulting cDNA was used in a PCR with the tag sequence and F15 as primers[38,39]. We tested all *Bombus* samples that were positive for DWV presence and, where possible, two DWV-positive *Apis* samples from each site where we found DWV in *Bombus*.

Sequencing. DWV sequence diversity was analysed by sequencing up to five independent clones per *Bombus* samples infected with negative-strand DWV from five sites (H, L, Q, R, X; chosen for their high DWV-infection prevalence in *Bombus*) and five clones of DWV-infected *Apis* samples from the same sites (we checked extra *Apis* samples for DWV infection, if necessary, to match *Bombus* DWV infections). All *Bombus* samples were *B. lapidarius*, with the exception of one sample from site L (clone 05), which was *B. pascuorum* (this sample is not included in any of the other analyses, but revealed a DWV infection in an initial screening and was hence included in the virus variant analysis). We sequenced a region of the DWV genome: the RNA-dependent RNA polymerase gene (F15–B23 primer pair[35] used throughout the study).

RNA-dependent RNA polymerase is thought to be a conserved region of the virus genome in which non-synonymous substitutions may have significant implications for the epidemiology of the virus[24]. RT–PCRs and PCR were run as described before. DWV PCR products were verified by gel electrophoresis as described above; if a clear, clean single band was visible, we proceeded directly to the cloning protocol. If not, we purified products from the agarose gel following a standard protocol (Qiaquick Gel Extraction Kit, Qiagen) and used the purified fragment in an additional PCR. PCR products were cloned using the Invitrogen TA cloning kit (Invitrogen), according to the manufacturer's instructions. Plasmid DNA was isolated using the Spin Miniprep kit (Qiagen) and the successful insertion of target sequence was tested by restriction analysis (digested with EcoRI). Up to five clones per sample were sequenced in forward and reverse orientation (Source BioSciences).

Analysis of DWV sequences. The 75 *Apis* and *Bombus* clones from sites H, L, Q, R and X were supplemented with DWV and VDV reference RNA-dependent RNA polymerase sequences (accession numbers NC004830 and NC006494, respectively), resulting in a final alignment of 420 bp from 77 sequences. Forward and reverse sequences of each clone were assembled and the consensus sequence was used for further analysis. Sequences were aligned using Geneious (R 6.1.6) with standard settings. Ends were trimmed by hand. For the tree building we conducted two independent (MC)³ algorithms running for two-million generations, each with four chains (three hot, one cold), sampling 1 tree in 1,000, under the GTR + Γ (generalised time reversible model of sequence evolution with a gamma distribution)

(Nst (number of substitution types) = 6) substitution model. Gene trees were estimated using PhyML v.3.0 (ref. 40) maximum-likelihood (ML) bootstrapping (500 replicates) and MrBayes v3.2.1 (ref. 41), under a GTR + Γ model, using four categories to accommodate rate variation across sites. Burn-in cutoffs (the time given for the tree sampling to converge to its stationary phase, to determine the trees removed prior to analysis) were inspected manually for each parameter file in Tracer v1.5 (ref. 42). Inspection of the standard deviation of split frequencies confirmed that the trees sampled in both $(MC)^3$ runs had converged (0.0093). To test alternative a priori hypotheses of virus diversification, for each virus (DWV and VDV) we constrained clades according to site (H, L, Q, R and X) or host genus (Apis and Bombus), and performed stepping stone sampling[23] as implemented in MrBayes v3.2.1 to estimate marginal log likelihoods. Sampling was conducted for 50 steps of 39,000 generations for two independent MCMC runs to ensure that accurate estimates were obtained. The first 9,000 generations of every step were discarded as burn-in. The model with the highest likelihood score was used as the null hypothesis. We compared Bayes factors for both models and used a threshold of 2 ln (Bayes factors) > 10 as decisive support for the null against the alternative hypothesis[43] (Extended Data Table 2). We repeated stepping-stone sampling to confirm run stability (data not shown).

Statistics. Mean survival of control treatments, free of the two test pathogens, was 14.2 ± 4.2 days (mean ± s.d.), whereas DWV-treated bees survived for 8.1 ± 5.8 days (mean ± s.d.). To assess the effect of infection on survival we fitted a Cox mixed effects model with treatment as a fixed factor and colony of origin as a random factor and compared it to the null model[44] (R library coxme, version 2.2-3, function coxme). The model was fitted with the penalized partial likelihood (PPL) and showed a significant negative impact of infection on longevity ($X^2 = 11.93$, d.f. = 4.17; $P < 0.021$).

$N.$-ceranae-treated bees survived for 18 ± 1 days (mean ± s.d.). A model with treatment as a fixed factor and colony of origin as a random factor showed no improvement over the null model (PPL: $X^2 = 0.12$, d.f. = 1; $P > 0.735$).

True prevalences with 95% confidence intervals were computed to correct for varying sample sizes (owing to the different species of bumblebee at the sampling sites) and test sensitivity was set to a conservative 95% (ref. 45). Confidence-interval estimates are based on a previous method for exact two-sided confidence intervals[46] for each sampling site and for each species sampled[47] (R library epiR, version 0.9-45, function epi.prev).

To investigate our spatially distributed data set we undertook an exploratory data analysis (EDA)[48] in which we calculated a prevalence surface for each of our parasites using Gaussian kernel estimators with an adaptive bandwidth of equal number of observations. This is a variant of the nearest neighbour technique, with bandwidth size being determined by a minimum number of observations in the neighbourhood (set to three times the maximum observations per site)[49] (R library prevR, version 2.1, function kde). Estimated surfaces were used for visual inspection only (Fig. 2); all the remaining analyses are based on the raw data only.

To investigate spatial structure and disease hotspots we used spatial autocorrelation statistics of the true prevalence of each of the pathogens in the different host genera from the 26 collection sites. To identify whether or not the pathogens we found were spatially clustered, we computed the spatial autocorrelation coefficient Moran's I^{50} with an inverse spatial distance weights matrix, as implemented in Gittleman and Kot[51] (R library ape, version 3.0-7, function Moran.I)[52]. Moran's I is a weighted measure describing the relationship of the prevalence values associated with spatial points. The coefficient ranges from -1 (perfect dispersion) through 0 (no spatial autocorrelation (random distribution)) to 1 (perfect clustering).
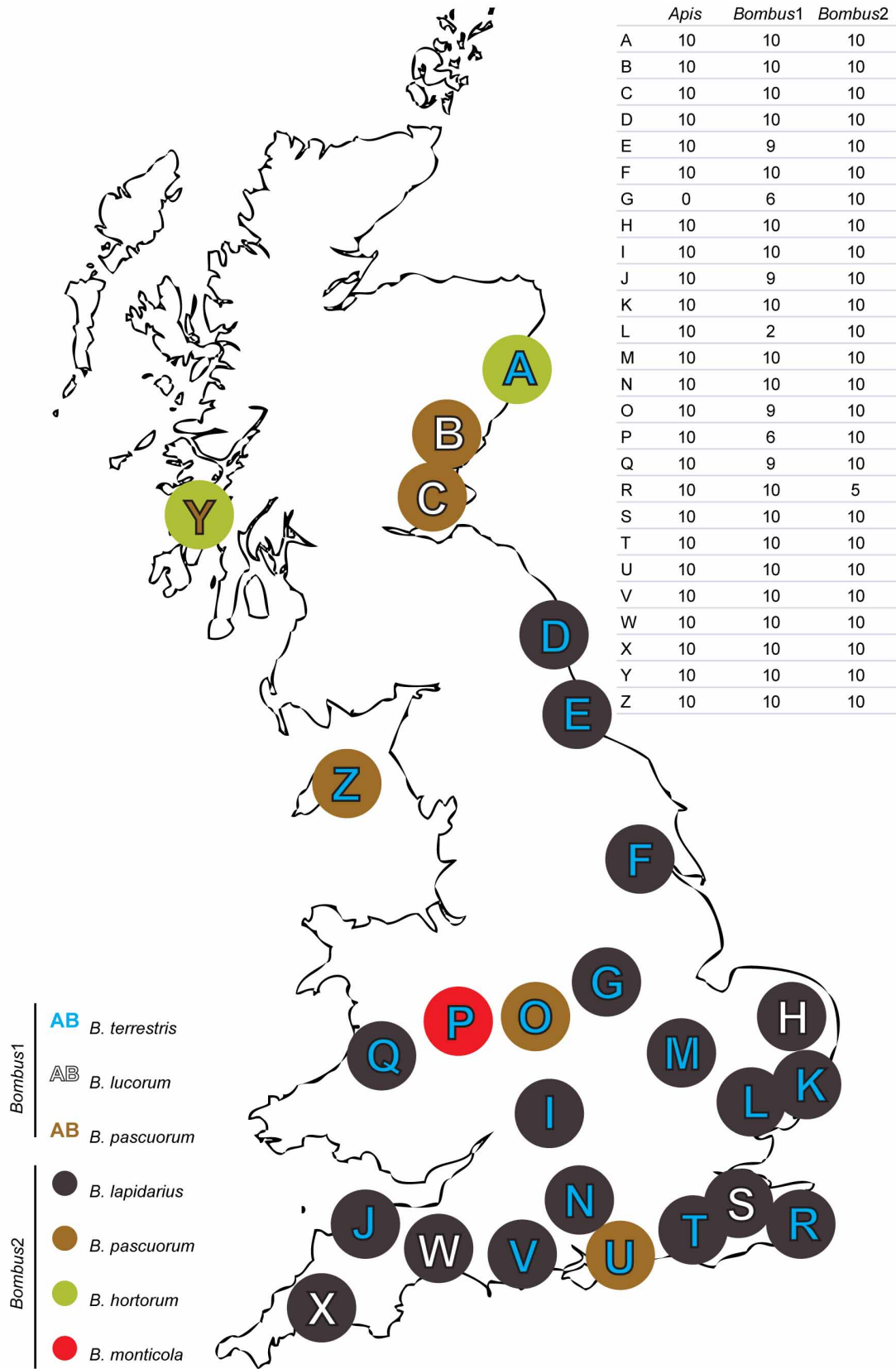
To investigate whether pathogen prevalence (Nosema and DWV were tested in separate models) in Apis, Bombus:Apis (ratio of host densities), or Apis absolute abundance had an effect on pathogen prevalence in Bombus, we ran a generalized linear mixed model (GLMM)[53] with binomial error structure and logit link function using the function lmer of the R package lme4 (ref. 54). Latitude, longitude, sunlight hours (a proxy for favourable foraging weather that would enable disease transmission; calculated cumulatively from March until the month of collection (data were collected from the MET office webpage: http://www.metoffice.gov.uk/ climate/uk/anomacts/, averaging over area sunlight-hour-ranges)) and landcover type were included in the model as fixed control effects (present in the full as well as the null model), and site and species were included in the model as random effects (present in the full as well as the null model). Before running the model we inspected all predictors for their distribution, as a consequence of which we log transformed 'Bombus:Apis' and 'Apis abundance' to provide more symmetrical distributions. Thereafter, we z-transformed all quantitative predictors to a mean of zero and a standard deviation of one to derive more comparable estimates and to aid interpretation of interactions[55]. As changes in 'Bombus:Apis' and 'Apis abundance' could lead to changes in pathogen prevalence in Bombus because of a change in pathogen prevalence in Apis, we included the interactions between 'Bombus:Apis' and pathogen prevalence in Apis, and 'Apis abundance' and pathogen prevalence

in Apis. To test the overall effect of our three test predictors, we compared the full model with a reduced model (null model) using a likelihood ratio test comprising latitude, longitude, sunlight hours and landcover type with the same random effects structure. Model stability was assessed by excluding data points one by one and comparing the estimates derived from these reduced models with estimates from the full model (revealing a stable model). Site G had to be excluded from this analysis as no Apis samples were found on site.

We fitted linear models to assess the relationships of parasite prevalence among Apis and Bombus.

We investigated the effect of pathogen treatment on disease status of an individual with a GLMM[53] with binomial error structure and logit link function using the function lmer of the R package lme4 (ref. 54). Colony of origin was entered into the model as a random effect. As described before, we checked model stability (the model with interaction terms included was unstable; however it stabilized once the non-significant interaction terms were removed), before testing the full model against the null model using a likelihood-ratio test. All analyses were run in R (ref. 56).

29. Higes, M., Martin-Hernandez, R., Garrido-Bailon, E., Garcia-Palencia, P. & Meana, A. Detection of infective Nosema ceranae (Microsporidia) spores in corbicular pollen of forager honeybees. J. Invertebr. Pathol. **97,** 76–78 (2008).
30. Cole, R. J. Application of the ''triangulation'' method to the purification of Nosema spores from insect tissues. J. Invertebr. Pathol. **15,** 193–195 (1970).
31. Bailey, L. L. & Ball, B. V. Honey bee pathology 2nd edn, (Academic Press, 1991).
32. Yañez, O. et al. Deformed wing virus and drone mating flights in the honey bee (Apis mellifera): implications for sexual transmission of a major honey bee virus. Apidologie **43,** 17–30 (2012).
33. Murray, T. E., Fitzpatrick, U., Brown, M. J. F. & Paxton, R. J. Cryptic species diversity in a widespread bumble bee complex revealed using mitochondrial DNA RFLPs. Conserv. Genet. **9,** 653–666 (2008).
34. Chen, Y., Evans, J. D., Smith, I. B. & Pettis, J. S. Nosema ceranae is a long-present and wide-spread microsporidian infection of the European honey bee (Apis mellifera) in the United States. J. Invertebr. Pathol. **97,** 186–188 (2008).
35. Genersch, E. Development of a rapid and sensitive RT-PCR method for the detection of deformed wing virus, a pathogen of the honeybee (Apis mellifera). Vet. J. **169,** 121–123 (2005).
36. Hornáková, D., Matouskova, P., Kindl, J., Valterova, I. & Pichova, I. Selection of reference genes for real-time polymerase chain reaction analysis in tissues from Bombus terrestris and Bombus lucorum of different ages. Anal. Biochem. **397,** 118–120 (2010).
37. de Miranda, J. R. & Genersch, E. Deformed wing virus. J. Invertebr. Pathol. **103,** S48–S61 (2010).
38. Yue, C. & Genersch, E. RT-PCR analysis of deformed wing virus in honeybees (Apis mellifera) and mites (Varroa destructor). J. Gen. Virol. **86,** 3419–3424 (2005).
39. Craggs, J. K., Ball, J. K., Thomson, B. J., Irving, W. L. & Grabowska, A. M. Development of a strand-specific RT-PCR based assay to detect the replicative form of hepatitis C virus RNA. J. Virol. Methods **94,** 111–120 (2001).
40. Guindon, S. et al. New algorithms and methods to estimate maximum-likelihood phylogenies: assessing the performance of PhyML 3.0. Syst. Biol. **59,** 307–321 (2010).
41. Huelsenbeck, J. P. & Ronquist, F. MRBAYES: Bayesian inference of phylogenetic trees. Bioinformatics **17,** 754–755 (2001).
42. Rambaut, A. & Drummond, A. J. Tracer v1.5 http://beast.bio.ed.ac.uk/Tracer (30 November 2009).
43. de Bruyn, M. et al. Paleo-drainage basin connectivity predicts evolutionary relationships across three southeast Asian biodiversity hotspots. Syst. Biol. **62,** 398–410 (2013).
44. Therneau, T. Coxme: Mixed Effects Cox Models http://CRAN.R-project.org/ package=coxme (15 May 2012).
45. Reiczigel, J., Foldi, J. & Ozsvari, L. Exact confidence limits for prevalence of a disease with an imperfect diagnostic test. Epidemiol. Infect. **138,** 1674–1678 (2010).
46. Blaker, H. Confidence curves and improved exact confidence intervals for discrete distributions. Can. J. Statist. **28,** 783–798 (2000).
47. epiR:. an R package for the analysis of epidemiological data v. R package version 0.9-45 (30 November 2012).
48. Rossi, R. E., Mulla, D. J., Journel, A. G. & Franz, E. H. Geostatistical tools for modeling and interpreting ecological spatial dependence. Ecol. Monogr. **62,** 277–314 (1992).
49. Larmarange, J., Vallo, R., Yaro, S., Msellati, P. & Meda, N. Methods for mapping regional trends in HIV prevalence from demographic and health surveys (DHS). Cybergeo. http://cybergeo.revues.org/24606 (2011).
50. Moran, P. A. Notes on continuous stochastic phenomena. Biometrika **37,** 17–23 (1950).
51. Gittleman, J. L. & Kot, M. Adaptation: statistics and a null model for estimating phylogenetic effects. Syst. Biol. **39,** 227–241 (1990).
52. Paradis, E., Claude, J. & Strimmer, K. APE: Analyses of phylogenetics and evolution in R language. Bioinformatics **20,** 289–290 (2004).
53. Baayen, R. H., Davidson, D. J. & Bates, D. M. Mixed-effects modeling with crossed random effects for subjects and items. J. Mem. Lang. **59,** 390–412 (2008).
54. Bates, D., Maechler, M. & Bolker, B. lme4: Linear mixed-effects models using S4 classes (22 June 2012).
55. Schielzeth, H. Simple means to improve the interpretability of regression coefficients. Meth. Ecol. Evol. **1,** 103–113 (2010).
56. R Foundation for Statistical Computing R: a language and environment for statistical computing (26 October 2012).

	Apis	Bombus1	Bombus2
A	10	10	10
B	10	10	10
C	10	10	10
D	10	10	10
E	10	9	10
F	10	10	10
G	0	6	10
H	10	10	10
I	10	10	10
J	10	9	10
K	10	10	10
L	10	2	10
M	10	10	10
N	10	10	10
O	10	9	10
P	10	6	10
Q	10	9	10
R	10	10	5
S	10	10	10
T	10	10	10
U	10	10	10
V	10	10	10
W	10	10	10
X	10	10	10
Y	10	10	10
Z	10	10	10

Bombus1

AB *B. terrestris*

AB *B. lucorum*

AB *B. pascuorum*

Bombus2

● *B. lapidarius*

● *B. pascuorum*

● *B. hortorum*

● *B. monticola*

Extended Data Figure 1 | Host bee species and sampling-site distributions. Distribution of sampling sites across Great Britain and the Isle of Man. The most common *Bombus* species on a given site is represented by coloured letters and the second most common *Bombus* species is represented by the colours of the dots. Total sample sizes for each site are given in the table.
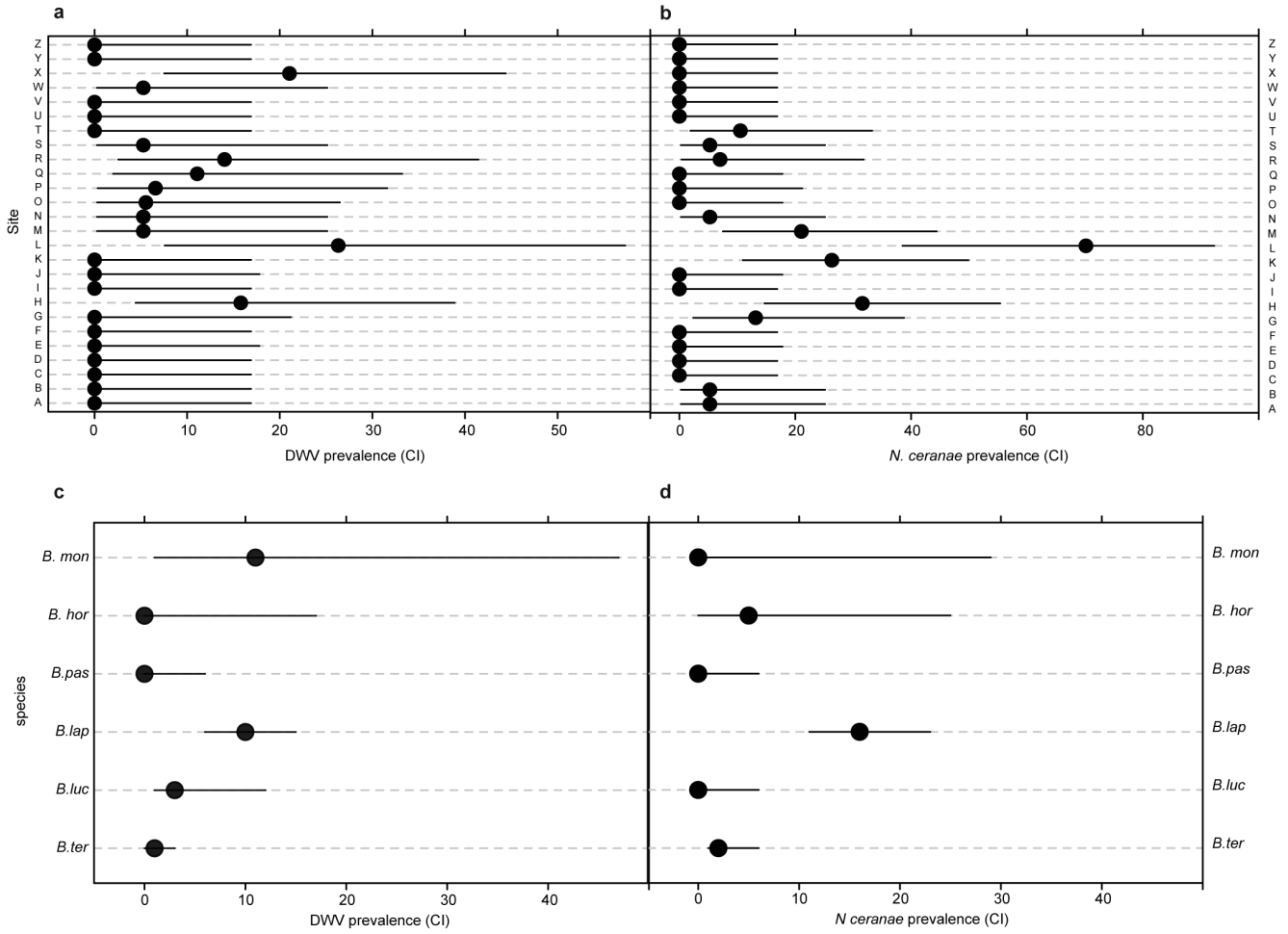
Extended Data Figure 2 | Prevalence of DWV and *N. ceranae* per site and host bee species. a–d, Pathogen prevalence in *Bombus* spp. in per cent per site for DWV (**a**) and for *N. ceranae* (**b**), and per species for DWV (**c**) and for *N. ceranae* (**d**). Bars indicate 95% confidence intervals. Note different scales.
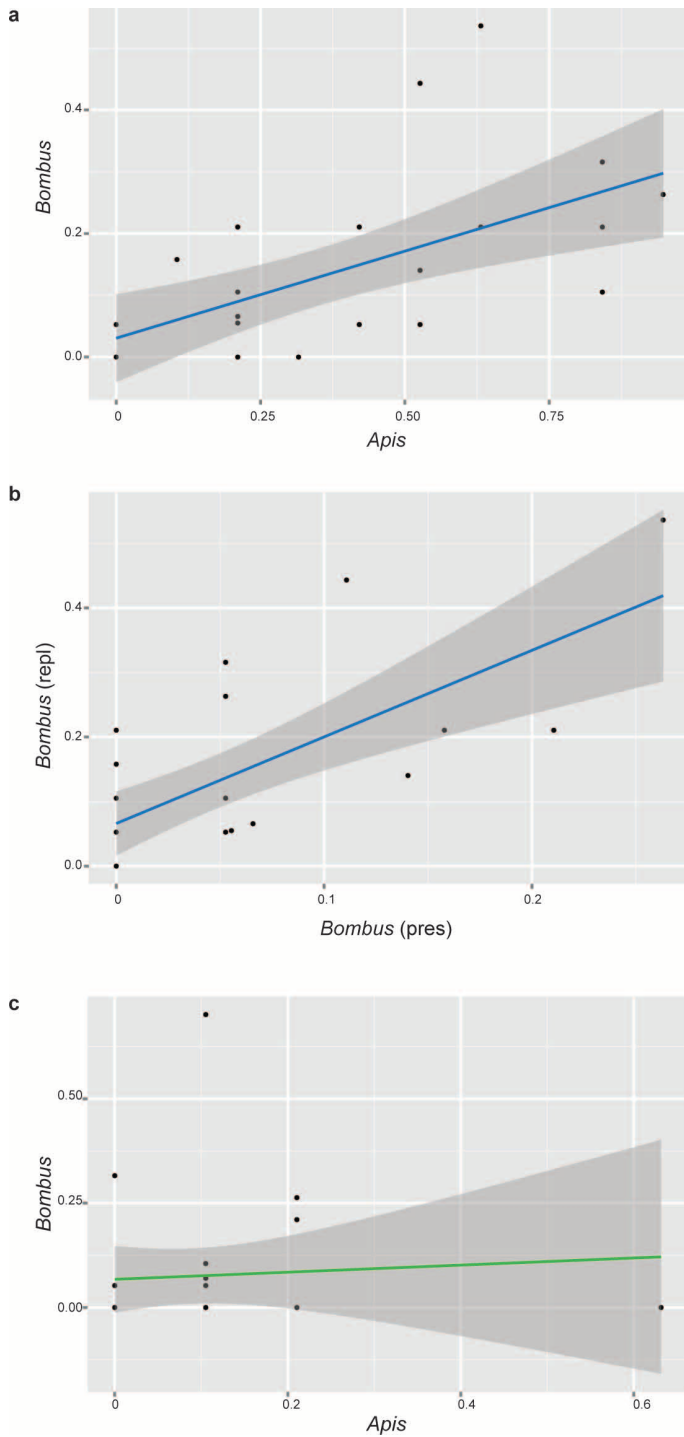
Extended Data Figure 3 | Raw data for prevalence of DVW and *N. ceranae*. The linear models shown only illustrate the relationships but do not drive the conclusions in the main text. **a**, DWV presence in *Apis* and *Bombus* (adjusted $R^2 = 0.34$, $P < 0.001$). **b**, DWV replicating in *Bombus* and DWV presence in *Bombus* (adjusted $R^2 = 0.46$, $P < 0.001$). **c**, *N. ceranae* presence in *Apis* and *Bombus* (adjusted $R^2 = -0.04$, $P > 0.728$). The line shows the best fit and the dark grey region shows 95% confidence interval of fit.

Extended Data Table 1 | Pathogen prevalence per species

species (N)	Apis (250)	B.ter (170)	B.luc (60)	B.lap (175)	B.pas (60)	B.hor (20)	B.mon (10)
DWV present	36 [30, 43]	9 [5, 14]	18 [9, 29]	16 [11, 23]	4 [1, 12]	0 [0, 17]	11 [1, 47]
DWV replicating	88 [70, 98]*	1 [0, 3]	4 [1, 12]	10 [6, 15]	0 [0, 6]	0 [0, 17]	11 [1, 47]
N. ceranae	9 [6, 13]	2 [1, 6]	0 [0, 6]	16 [11, 23]	0 [0, 6]	5 [0, 25]	0 [0, 29]
single infection	18 [14, 23]	3 [1, 7]	3 [1, 12]	20 [14, 27]	0 [0, 6]	5 [0, 25]	11 [1, 47]
co-infection	1 [0, 3]	0 [0, 2]	0 [0, 6]	3 [1, 7]	0 [0, 6]	0 [0, 17]	0 [0, 29]

* The number given is out of the 31 DWV-present *Apis* samples tested. Pathogen prevalence is given in per cent with 95% confidence intervals [% prevalence, 95% confidence interval range]. Sample numbers (N) are shown in brackets.

Extended Data Table 2 | Alternative models for the diversification of DWV and VDV viruses in UK pollinators

Model		Marginal likelihood (ln)	Difference	BF	2 ln (BF)	Preferred model
Site (S)	Null	-1512.71				
			-94.92	$>10^{41}$	189.84	S
Host (H)		-1607.63				

The preferred tree model (Site) as determined by Bayes factor (BF) comparison.